Available online at www.sciencedirect.com
ScienceDirect
Ceramics International 37 (2011) 2025–2029
CERAMICS INTERNATIONAL
www.elsevier.com/locate/ceramint

Short communication

Hydroxyapatite/diopside ceramic composites and their behaviour in simulated body fluid

Mufan Zhang [a], Changxia Liu [b], Junlong Sun [b], Xihua Zhang [c,*]

[a] School of Medicine, Shandong University, Jinan 250012, Shandong Province, PR China
[b] Key Laboratory of Advanced Manufacturing and Automation Technology, Ludong University, Yantai 264025, Shandong Province, PR China
[c] School of Materials Science and Engineering, Shandong University, Jinan 250061, Shandong Province, PR China

Received 23 June 2010; received in revised form 17 December 2010; accepted 22 January 2011
Available online 18 February 2011

Abstract

In this work, diopside was introduced in hydroxyapatite matrix as a sintering aid and hydroxyapatite/diopside ceramic composites were fabricated by uniaxial hot-pressing. The biological activity of hydroxyapatite/diopside ceramic composites in simulated body fluid was assessed by means of scanning electron microscopy (SEM), thin-film X-ray diffraction (TF-XRD) and electron-probe micro analysis (EPMA). SEM micrographs showed an obvious bright mineral layer to form on the soaked composite surface, and the layer may be hydroxyapatite or NaCl crystals.

Keywords: Hydroxyapatite; Diopside; Biological activity

1. Introduction

Calcium phosphate ceramic such as hydroxyapatite is good candidate for bone tissue regeneration in biomedical industries due to their biocompatibility, low density, chemical stability and their compositional similarity to human bone. Unfortunately, the fracture toughness of pure hydroxyapatite does not exceed the value of about 1 MPa $m^{1/2}$ as compared with 2–12 MPa $m^{1/2}$ for human bone. Therefore, pure hydroxyapatite cannot be used as heavy-loaded implants such as artificial teeth or human bone [1]. Nowadays there have been a number of studies are reporting on additives to improve the fracture toughness of pure hydroxyapatite [2–6]. Improved mechanical properties are obtained owing to the incorporation of second phases such as ZrO_2 [2], SiCw [5] and Al_2O_3 [6] into hydroxyapatite, the biological activities of these fabricated hydroxyapatite matrix ceramic composites, however, decrease mainly due to the decomposition of hydroxyapatite during the sintering and subsequent formation of tricalcium phosphate (TCP) or CaO, which may increase the biodegradability of hydroxyapatite matrix ceramic composites [1].

Along with the advances in clinical applications, more and more hydroxyapatite matrix ceramic composites with good mechanical properties and biological activities are used in clinic for filling of bone defects. Unfortunately, the application of hydroxyapatite matrix ceramic composites is limited due to their high cost. So how to find low cost second phases has been a promising approach to produce high performance hydroxyapatite matrix ceramic composites with low cost. Diopside ($MgCa(SiO_3)_2$) just has the virtue of low-cost by contrast to other additives. It is reported that diopside can act as an accessory ingredient in the sintering process and decreases the sintering temperature of alumina matrix ceramic materials [7,8].

Our previous results showed that introduction of diopside in hydroxyapatite matrix ceramic composites can improve their bending strength and fracture toughness, and composites with high ratio of performances versus cost was obtained for advanced biomaterials [9]. However, there are few reports about the biological activity of hydroxyapatite/diopside ceramic composites in recent years. In this paper, the biological activities of hydroxyapatite/diopside ceramic composites in simulated body fluid are discussed.

* Corresponding author. Tel.: +86 13864000265.
E-mail address: hester5371@yahoo.com.cn (X. Zhang).

0272-8842/$36.00
doi:10.1016/j.ceramint.2011.01.045

Table 1
Starting compositions and mechanical properties of hydroxyapatite/diopside ceramic composites.

Specimens	Compositions (wt. %)		Mechanical properties		
	Diopside	Hydroxyapatite	Vickers hardness (GPa)	Flexural strength (MPa)	Fracture toughness (MPa $m^{1/2}$)
D_0	0	100	6.0 ± 2.5	27 ± 3	0.9 ± 0.1
D_{10}	10	90	5.4 ± 1.0	80 ± 5	1.2 ± 0.3

2. Experimental procedure

2.1. Preparation and characterization of hydroxyapatite/diopside ceramic composites

Hydroxyapatite of high purity (99%) and small grain size (1–3 μm) produced by Department of Materials Science and Engineering in Shandong University, was used as the starting material. Commercial diopside ($MgCa(SiO_3)_2$), composed of SiO_2 (55 wt.%), CaO (24 wt.%) and MgO (18 wt.%), was used as an additive. The raw materials were blended with each other according to their proportions listed in Table 1. Milling was carried out for 100 h in alcohol using a vibratory ball mill with cemented carbide balls and then metal-mill media impurities were removed by washing in 10 mol% hydrochloric acid. After drying, densification of the powder was achieved in a graphite die by uniaxial hot-pressing at 1310 °C, at a pressure of 28 MPa in a N_2 atmosphere for 30 min.

The sintered bodies were cut into bars and then standard test pieces (3 mm × 4 mm × 36 mm) were ground and polished with diamond paste. Three-point-bending mode was used to measure the bending strength using an electronic universal experimental instrument (Jinan Test Co., Ltd.) with a span of 20 mm at a crosshead speed of 0.5 mm/min. At least twelve specimens were tested for each series of composition in air at room temperature. Hardness was measured on the polished surfaces with a load of 9.8 N for 5 s using a micro-hardness tester (Shanghai Hengyi Electronic Testing Instrument Corporation). Fracture toughness measurements were performed using indentation method. The indentations on polished surfaces were generated by the Vickers micro-hardness tester with a diamond pyramid indenter, at a load of 196 N and a loading time of 30 s. The formula proposed by Cook and Lawn [10] was used to calculate the final fracture toughness. Data of hardness and fracture toughness were determined using at least 10 indentations on polished surfaces with a Ra of 0.1 μm for each specimen. The starting compositions and mechanical properties of hydroxyapatite/diopside ceramic composites are listed in Table 1.

2.2. Ability of hydroxyapatite/diopside ceramic composites to form an apatite layer

An acellular simulated body fluid (SBF) was used for in vitro experiments. SBF containing ion concentrations similar to those in human blood plasma was prepared according to the method described by Kokubo [11]. Briefly, reagent-grade $CaCl_2{\cdot}2H_2O$, $K_2HPO_4{\cdot}3H_2O$, NaCl, KCl, $MgCl_2{\cdot}6H_2O$, $NaHCO_3$, Na_2SO_4 and $(CH_2OH)_3CNH_2$ were dissolved in distilled water and adjusted to pH 7.4. Hydroxyapatite/diopside ceramic bars were soaked in SBF at 37 °C for 9 days. 100 ml of SBF was used for each bar. After soaking, the bars were washed with distilled water and dried at 100 °C for 0.5 days. The microstructure of the specimens was studied on the original polished surfaces and on the soaked bar surfaces by scanning electron microscope (HITACHI S-570). The phases of the soaked hydroxyapatite/diopside ceramic composites were determined by Thin-film X-ray diffraction (*D*/max-2400). The elements analysis in the microzone on the surfaces of the soaked hydroxyapatite/diopside ceramic composites was detected by EPMA (JXA-8800R)

3. Results and discussion

3.1. Microstructures of hydroxyapatite/diopside ceramic composites

SEM photographs of the D_0 specimen before and after soaking in SBF for 9 days are shown in Figs. 1–3. Those of the D_{10} specimen before and after soaking in SBF for 9 days are shown in Figs. 4–6. The polished surfaces of D_0 and D_{10} specimens before soaking in SBF were smooth and there existed some pores (Figs. 1 and 4). Compared with the polished surfaces of D_0 and D_{10} specimens before soaking in SBF, there were obvious bright mineral layers formed on the polished surfaces of D_0 and D_{10} specimens after soaking in SBF for

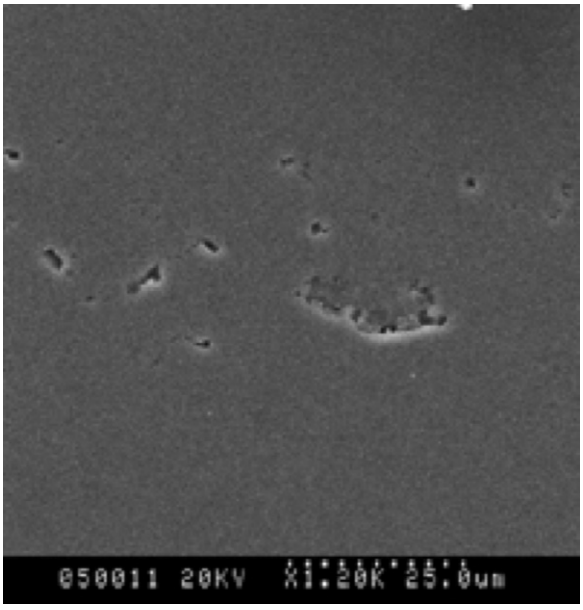

Fig. 1. SEM micrograph of D_0 specimen before soaking in SBF (1200×).

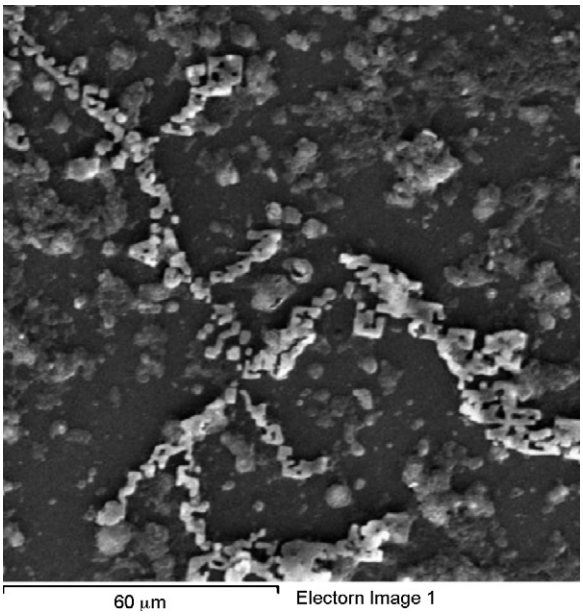

Fig. 2. SEM micrograph of D_0 specimen after soaking in SBF for 9 days (800×).

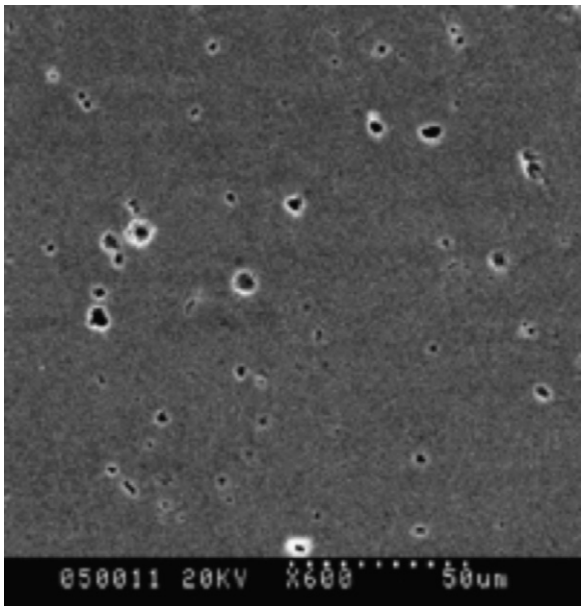

Fig. 4. SEM micrograph of D_{10} specimen before soaking in SBF (600×).

9 days (Figs. 2, 3, 5 and 6). The bright mineral layers formed on surfaces of the D_{10} specimen (Figs. 5 and 6) were thicker and more uniform than those formed on surfaces of the D_0 specimen (Figs. 2 and 3). In order to detect the phases of the bright mineral layers formed on the composite surfaces, the specimens were characterized by Thin-film X-ray diffraction (TF-XRD) and EPMA, respectively.

3.2. Thin-film X-ray diffraction (TF-XRD) analysis

TF-XRD patterns of the D_0 and D_{10} specimen after soaking in SBF for 9 days are shown in Figs. 7 and 8. It can be seen that there only existed hydroxyapatite in the soaked D_0 specimen (Fig. 7) and there existed hydroxyapatite, SiO_2, $CaSiO_3$ in the soaked D_{10} specimen (Fig. 8). In Fig. 8 there were no trace of CaO, which may react with SiO_2, leading to interface reactions and strengthened grain boundaries [12]. MgO was not found in Fig. 8 for the reason that the content of MgO was too small to be detected by XRD. By a comparison with our previous studies on XRD patterns of the D_0 and D_{10} specimen before soaking in SBF [12], the conclusion can be drawn that the bright mineral layers formed on the polished surfaces of the D_0 and D_{10} specimen after soaking in SBF for 9 days may be hydroxyapatite.

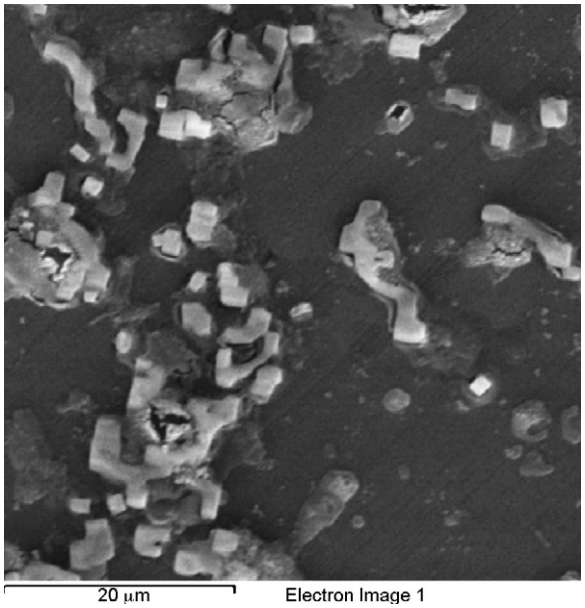

Fig. 3. SEM micrograph of D_0 specimen after soaking in SBF for 9 days (2000×).

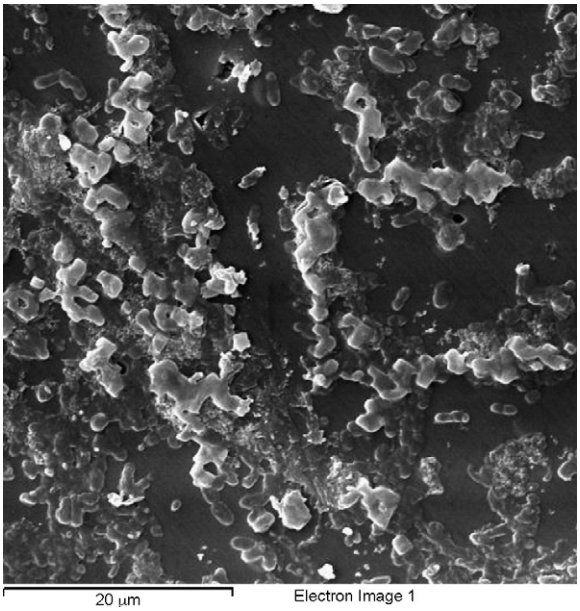

Fig. 5. SEM micrograph of D_{10} specimen after soaking in SBF for 9 days (2000×).

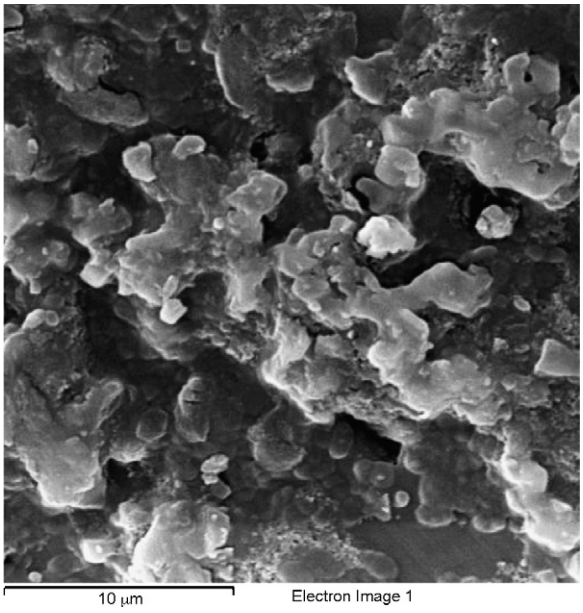

Fig. 6. SEM micrograph of D_{10} specimen after soaking in SBF for 9 days (4000×).

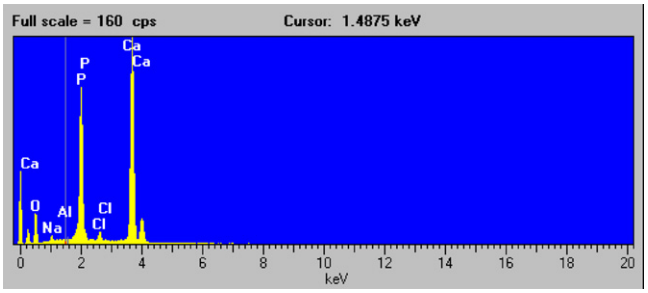

Fig. 9. EDS spectra of the D_0 specimen after soaking in SBF for 9 days.

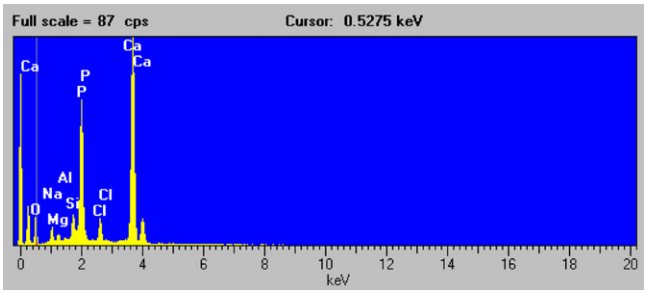

Fig. 10. EDS spectra of the D_{10} specimen after soaking in SBF for 9 days.

3.3. Electron-probe micro analysis (EPMA)

EDS spectra of the D_0 and D_{10} specimen after soaking in SBF for 9 days are shown in Figs. 9 and 10, respectively. Ca, P, Na and Cl appeared on the surfaces of D_0 and D_{10} specimen after soaking in SBF for 9 days. Therefore, one conclusion can be drawn that the phase of bright mineral layers may be hydroxyapatite, and the other can be drawn that the phase of bright mineral layers may be NaCl crystals formed on drying after extraction from SBF and poor washing. NaCl was not found in Figs. 7 and 8 for the reason that the content of NaCl is too small to be detected by XRD.

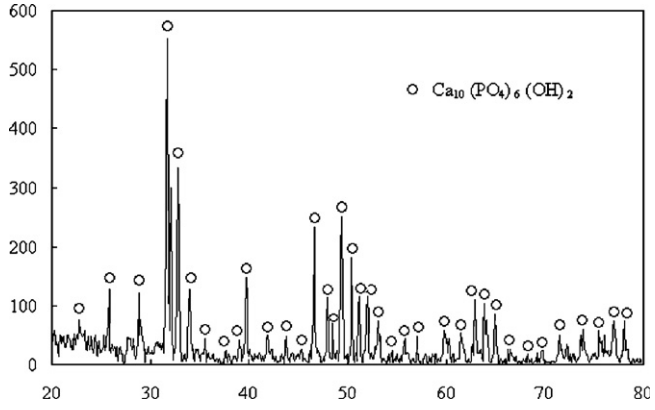

Fig. 7. TF-XRD patterns of the D_0 specimen after soaking in SBF for 9 days.

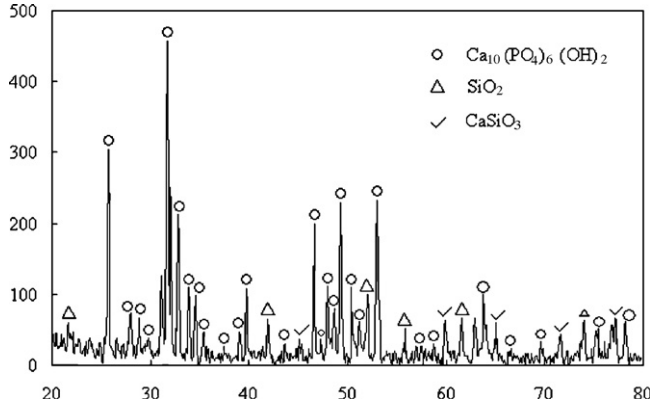

Fig. 8. TF-XRD patterns of the D_{10} specimen after soaking in SBF for 9 days.

In vitro test behaviour confirmed that the bright mineral layers formed onto the surfaces of pure hydroxyapatite and hydroxyapatite/diopside ceramic composites soaked in SBF for 9 days. SEM examination, EPMA and TF-XRD analyses showed the bright mineral layers may be a small quantity of NaCl crystals and a large amount of hydroxyapatite, which has a similar mineral composition to human bones [13,14]. Kokubo et al. [15,16] reported silica to play an important role for the nucleation and growth mechanism of the apatite-like layer on bioactive composites. In our study, an interchange is suggested to take place between the Ca^{2+} ions of hydroxyapatite/diopside ceramic composites and the H_3O^+ of the simulated body fluid, which may promote the formation of Si–OH groups on the hydroxyapatite/diopside ceramic composites surface and induce the apatite nucleation. The nuclei thus formed grow at the expense of the ions in the solution that has been saturated with respect to apatite. Therefore, the silica seems to be very important in increasing the in vitro bioactive behaviour of the fabricated hydroxyapatite/diopside ceramic composites.

4. Conclusions

Hydroxyapatite/diopside ceramic composites with good mechanical properties and expected good biological activity were fabricated by uniaxial hot-pressing. SEM showed bright

mineral layers formed on the composite surfaces. The bright mineral layers were composed of a small quantity of NaCl crystals and a large amount of hydroxyapatite, which was detected by EPMA and TF-XRD analyses. The results revealed that the fabricated composites with high performance versus cost ratio have the ability of inducing hydroxyapatite to deposit on the surfaces of the specimens.

Acknowledgements

The work described in this paper is supported by the Natural Science Foundation of Shandong Province (No. Y2007F29), Independent Innovation Foundation of Shandong University, IIFSDU (No. 2009JC011) and the Specialized Personnel Invitation Rewards of Ludong University (Nos. LY20074302 and LY20074303).

References

[1] W. Suchanek, M. Yashima, M. Kakihana, M. Yoshimura, Hydroxyapatite ceramics with selected sintering additives, Biomaterials 18 (13) (1997) 923–933.
[2] H. Guo, K. AKhor, Y.C. Boey, X. Miao, Laminated and functionally graded hydorxyapatite/yttria stabilized tetragonal zirconia composites fabricated by spark plasma sintering, Biomaterials 24 (2003) 667–675.
[3] S. Nath, K. Biswas, B. Basu, Phase stability and microstructure development in hydroxyapatite-mullite system, Scripta Mater. 58 (2008) 1054–1057.
[4] A.R. Boccaccini, J.J. Blaker, V. Maquet, et al., Preparation and characterisation of poly (latide-co-glycolide) (PLGA) and PLGA/bioglass composite tubular foam scaffolds for tissue engineering applications, Mater. Sci. Eng. C 25 (2005) 23–31.
[5] Z. Niu, J. Zhang, S. Ren, et al., Effect of whisker orientation on mechanical properties of HAP-SiCw composite bioceramics, J. Mater. Sci. Eng. 23 (1) (2005) 1–3.
[6] J.H. Yih, H.M. Hsiung, Fabrication and mechanical properties of hydroxyapatite–alumina composites, Mater. Sci. Eng. C 2 (1–2) (1994) 77–81.
[7] C. Liu, J. Zhang, J. Sun, X. Zhang, Y. Hu, Addition of Al–Ti–C master alloys and diopside to improve the performance of alumina matrix ceramic materials, Ceram. Int. 33 (7) (2007) 1149–1154.
[8] J. Sun, C. Liu, X. Zhang, B. Wang, X. Ni, Effect of diopside addition on sintering and mechanical properties of alumina, Ceram. Int. 35 (4) (2009) 1321–1325.
[9] X. Zhang, C. Liu, M. Li, Y. Bai, J. Sun, Fabrication of hydroxyapatite/diopside/alumina composites by hot-press sintering process, Ceram. Int. 35 (5) (2009) 1969–1973.
[10] R.F. Cook, B.R. Lawn, A modified indentation toughness technique, J. Am. Ceram. Soc. 66 (11) (1983) 200–201.
[11] T. Kokubo, H. Kushitani, S. Sakka, T. Kitsugi, T. Yamamuro, Solutions able to reproduce in vivo surface-structure changes in bioactive glass–ceramic A-W, J. Biomed. Mater. Res. 24 (1990) 721–734.
[12] X. Zhang, C. Liu, M. Li, M. Xu, Y. Bai, Fabrication of hydroxyapatite/diopside composites by hot-press sintering process, J. Synth. Cryst. 36 (4) (2007) 837–840 (in Chinese).
[13] R. Manoharan, J.J. Baraga, R.P. Rava, R.R. Dasari, M. Fitzmaurice, M.S. Feld, Biochemical analysis and mapping of atherosclerotic human artery using FT-IR microspectroscopy, Atherosclerosis 103 (1993) 181–193.
[14] K. Schmid, W.O. McSharry, C.H. Pameijer, J.P. Binette, Chemical and physiochemical studies on the mineral deposits of the human atherosclerotic aorta, Atherosclerosis 37 (1980) 199–210.
[15] T. Kokubo, Novel bioactive materials, An Quim. Int. Ed. 93 (1997) 49–55.
[16] S. Padilla, J. Román, S. Sánchez-Salcedo, M. Vallet-Regí, Hydroxyapatite/SiO_2–CaO–P_2O_5 glass materials: in vitro bioactivity and biocompatibility, Acta Biomater. 2 (3) (2006) 331–342.